Supplementary Information

Rolling Circle Transcription-Amplified Hierarchically Structured Organic-Inorganic Hybrid RNA Flowers for Enzyme Immobilization

Ye Wang,[†] Eunjung Kim,[†] Yiyang Lin, Nayoung Kim, Worrapong Kit-Anan, Sahana Gopal, Shweta Agarwal, Philip D. Howes[a] and Molly M. Stevens*

Department of Materials, Department of Bioengineering and Institute of Biomedical Engineering, Imperial College London, London, SW7 2AZ, UK

[a]*Current Address: Department of Chemistry and Applied Biosciences, ETH Zürich, CH-8093 Zürich, Switzerland*

**E-mail: m.stevens@imperial.ac.uk (M.M. Stevens)*

[†]These authors contributed equally.

Materials: HPLC-purified oligonucleotides were purchased from Integrated DNA Technology (IDT, Belgium) and used without further purification. T4 DNA ligase, exonuclease I, T7 RNA polymerase (RNAP), and ribonucleotide triphosphates (rNTPs) solution mix were obtained from New England Biolabs (UK). Cyanine 5 (Cy5) and biotin conjugated-uridine triphosphate (Cy5-UTP or bio-UTP) were purchased from Enzo Life Sciences (UK). Dibenzocyclooctyne-modified UTP (DBCO-UTP) was purchased from Jena Bioscience (Germany). Avidin-Alexa Fluor™ 488 conjugate, fluorescence biotin quantitation kit, streptavidin-β-galactosidase conjugate, agarose, urea, Tris-HCl buffer (pH 8.0), Tris/boric acid/EDTA (TBE) buffer, 1 kb plus DNA ladder, SYBR gold stain, bluejuice gel loading dye, Quant-iT™ RiboGreen RNA assay kit, Qubit protein assay, PiPer pyrophosphate assay, nuclease-free water, and streptavidin-coated quantum dots with nominal emission of 605 nm (STV-QD_{605}) were obtained from Thermo Fisher Scientific (UK). TBE-urea sample buffer, 40% acrylamide/bis solution (29:1), and 30% acrylamide/bis solution (29:1) were purchased from Bio-Rad (USA). Amicon Ultra-0.5 Centrifugal Filter Units with Ultracel-10 membrane (MWCO 10 kDa) were purchased from MERCK Millipore (Germany). Cy3-azide conjugate, CdS_xSe_{1-x}/ZnS core-shell QDs (2 μM in toluene) with a nominal emission wavelength of 525 nm (QD_{525}) and 570 nm (QD_{570}), bovine serum albumin (BSA), horseradish peroxidase (HRP), and resorufin β-D-galactopyranoside (RBG) substrate, and Eppendorf RNA/DNA LoBind microcentrifuge tubes were obtained from Sigma Aldrich (UK). Azide- and biotin-modified QDs (N_3-QD_{525} and Bio-QD_{575}) were achieved through phase transfer with home-made ligand.[1]

Methods:

Preparation of Circular Template DNA: A circular template DNA was prepared following previous procedures.[2] Briefly, 5 μL of 5'-phosphorylated linear template DNA (100 μM) was circularized by hybridizing with 10 μL of T7 promoter (100 μM) in the ligase reaction buffer (50 mM Tris-HCl, 10 mM DTT, 1 mM ATP, 10 mM $MgCl_2$, pH 7.5) by heating at 95 °C for 5 min and slowly cooling to room temperature for at least 3 h. The sequences of oligonucleotides are as follows: linear template DNA, 5'- phosphorylation-TGA GTC GTA TTA TAG GCC TGC TCG AGC TCG AGC TTG CAT CAC CGT GCA GCC GAA GCT TGC ACG CGT A CCC TAT AG-3' and T7 promoter, 5'- TAA TAC GAC TCA CTA TAG GG-3'. The nick of the hybridized template DNA/T7 promoter was closed by adding 5 μL of T4 DNA ligase (400 U/μL) and incubating at 16 °C overnight, followed by enzyme inactivation at 65 °C for 10 min. 6 μL of exonuclease I (20 U/μL)

in reaction buffer (67 mM glycine-KOH, 6.7 mM $MgCl_2$, 10 mM β-mercaptoethanol, pH 9.5) was added to remove any free single-stranded DNA, and treated at 37 °C for 1.5 h before heat inactivation at 80 °C for 15 min. The resulting circularized template DNA was confirmed by both 15% native and denatured polyacrylamide gel electrophoresis (PAGE) analysis in TBE buffer (89 mM Tris-HCl, 89 mM boric acid, 2 mM EDTA, pH 8.3). To visualize DNA bands, the gels were stained with SYBR gold stain at room temperature for 30 min and imaged using the BioSpectrum Imaging System (Ultra-Violet Products, UK).

Synthesis of hRNFs Using RCT: In a typical rolling circle transcription (RCT) reaction, 50 µL solution containing circular template DNA (0.6 µM), rNTP mix (2 mM), T7 RNAP (5 U/µL), and BSA (200 µg/mL) was incubated in RCT reaction buffer (40 mM Tris-HCl, 6 mM $MgCl_2$, 2 mM spermidine, 1 mM DTT, pH 7.9) at 37 °C for 20 h. The T7 RNAP enzyme was inactivated at 65 °C for 10 min after the reaction. The final product was sonicated for 10 min, followed by washing with nuclease-free water several times to remove any free enzymes and RNA strands by centrifugation at 8,000 g for 10 min. The obtained hybrid RNA flowers (hRNFs) were redispersed in nuclease-free water and stored at 4 °C for use.

Quantification of RNA Concentration: The RNA content in hRNFs was quantified using Quant-iT™ RiboGreen RNA assay kit. The as-synthesized hRNFs were incubated with the RiboGreen reagent in a 96-well microplate for 5 min at room temperature. The fluorescence intensity (excitation at 480 nm, emission at 520 nm) was recorded using an EnSpire® Multimode plate reader (Perkin Elmer, UK). The RNA concentration was determined from the standard curve of serial dilutions of a ribosomal RNA standard provided by the manufacturer.

Quantification of PPi Concentration: The pyrophosphate (PPi) concentration was estimated using the PiPer pyrophosphate assay kit. The samples were mixed with a freshly prepared working solution containing Amplex Red (100 µM), pyrophosphatase (0.02 U/mL), maltose phosphorylase (4 U/µL), maltose (0.4 mM), glucose oxidase (2 U/mL), and horseradish peroxidase (0.4 U/µL), according to the manufacturer's protocols. After 2 h incubation at 37 °C, the absorbance at 565 nm was monitored using an EnSpire® Multimode plate reader (Perkin Elmer, UK) and inverted to PPi concentration using appropriate PPi standards.

Synthesis of Functional hRNFs: For synthesis of biotin- or DBCO-functionalized hRNF (Bio-hRNFs or DBCO-hRNFs), the RCT reaction was carried out with the addition of bio-UTP or

DBCO-UTP (40 μM) at 37 °C for 20 h before deactivation of T7 RNAP. For the preparation of avidin-functionalized hRNFs (Av-hRNFs), 10 μL of pre-synthesized hRNFs (RNA concentration = 50 μg/mL) was further complexed with 10 μL of avidin solution (50 μg/mL) at room temperature for at least 3 h. The resulting products were sonicated and washed with nuclease-free water three times by centrifugation at 8,000 g for 10 min. The obtained functional hRNFs (Bio-hRNFs, DBCO-hRNFs, and Av-hRNFs) were redispersed in nuclease-free water and stored at 4 °C for use.

SEM Imaging: The morphology and size distribution of the particles were analyzed using a Leo Gemini 1525 FEG scanning electron microscope (SEM) with a secondary electron in-lens detector at an accelerating voltage of 5 kV. To prepare the SEM sample, a drop of each sample solution in nuclease-free water was placed onto a cleaned silicon wafer chip and air-dried at room temperature, followed by sputter coating with 10 nm chromium in a Q150T S sputter coater (Quorum Technologies, UK).

STEM Imaging and STEM-EDS Analysis: Imaging in scanning transmission microscopy (STEM) mode and energy dispersive X-ray spectroscopy (EDS) analysis were performed on a JEOL JEM-2100F transmission electron microscope (TEM) operating at 200 kV, equipped with Gatan Orius SC 1000 (2k × 4k), Gatan high-angle annular dark-field (HAADF), and EDS detectors (Oxford Instruments INCA EDS 80 mm X-Max detector system with STEM capability). The samples were prepared by placing a drop of the sample solution on 200-mesh carbon-coated copper grids (Electron Microscopy Science, USA). For EDS analysis, measurements over five particles per sample were carried out. The relative atomic ratios normalized to Mg content in each particle were calculated through a standardless quantitative method with k-factors incorporated in the data processing software (Aztec Software, Oxford Instruments).

SIM Imaging: For structured illumination microscopy (SIM) imaging, fluorescently labeled-hRNF particles were prepared by additionally introducing Cy5-UTP (20 μM) to the RCT reaction mixtures, followed by the reaction at 37 °C for 20 h and purification in the same way as described above. For the imaging of QDs-labeled hRNFs, the pre-synthesized functional hRNF particles were first incubated with surface-modified QDs using a bench shaker at room temperature for 30–60 min, and then washed with nuclease-free water several times by centrifugation. 10 μL or more of the particles in nuclease-free water were mixed with 100 μL

of VectaShield mounting media (Vector Laboratories) before being pipetted onto an ibidi 8-well glass bottom μ-slide. The particles were left overnight in order to allow them to settle to the base of the slide by gravity. SIM imaging was performed with an Elyra PS.1 (Carl Zeiss).

Dual Beam FIB-SEM Analysis: Dual beam focused ion beam (FIB)-SEM imaging was carried out using Auriga CrossBeam Workstation (Zeiss). For imaging, samples were first fixed through resin embedding with an epoxy resin embedding kit (Sigma). A drop of sample solution in nuclease-free water was placed onto a cleaned silicon wafer chip and air-dried at room temperature. The chip was then incubated with a series of mixed ethanol and resin solution (volume ratio of ethanol to resin: 3:1, 2:1, 1:1, 1:2) for 2.5−3 h. The chip was washed with ethanol carefully to remove excess solution and air-dried between each step. The samples were left to polymerize for 48 h at 60 °C and finally coated with 10 nm chromium. A single particle was selected by SEM imaging at low magnification, followed by tilting the stage to 54°. The same particle was re-located using the FIB at a working distance of 5 mm. The sample was milled at 30 kV and 50 pA. SEM images were obtained under back-scattered electron (BSE) mode with an accelerating voltage of 1.6 keV.

Quantification of Biotin Concentration in Bio-hRNFs: The biotin concentration was measured using a Pierce™ biotin quantitation kit. The samples were mixed with a freshly prepared working solution according to the manufacturer's protocols, containing DyLight Reporter working reagent in PBS (2.7 mM KCl, 1.5 mM KH_2PO_4, 137 mM NaCl, 8.0 mM Na_2HPO_4, pH 7.4). After incubation in a 96-well microplate at room temperature for 5 min, the fluorescence intensity (excitation at 494 nm, emission at 520 nm) was measured using an EnSpire® Multimode plate reader (Perkin Elmer, UK). The biotin concentration was determined from the standard curve of serial dilutions of biocytin standard provided by the manufacturer.

Kinetics Study of STV-β-gal and STV-β-gal/Bio-hRNFs Complexes: Streptavidin-conjugated β-gal (STV-β-gal) at various concentrations (200, 400, and 600 ng/mL) was incubated with Bio-hRNFs at room temperature for 30 min. The resulting complexes were directly used for the kinetics study without further purification. In this experiment, we assumed that all enzymes were efficiently loaded onto Bio-hRNFs through biotin-avidin interactions. Enzyme kinetics study of STV-β-gal/Bio-hRNFs suspension and free STV-β-gal solution was performed in 50 μL of PBS buffer in the presence of RBG (400 μM). The fluorescence intensity (excitation at 550

nm, emission at 584 nm) was monitored at room temperature using an EnSpire® Multimode plate reader (Perkin Elmer).

Determination of the Michaelis-Menten Constants of STV-β-gal: The sample solution (STV-β-gal/Bio-hRNFs or STV-β-gal alone) and RBG substrates were mixed at a final concentration of 200 ng/mL STV-β-gal in PBS containing various concentrations of RBG (0, 50, 100, 200, 400, 600, and 800 μM). The fluorescence intensity (excitation at 550 nm, emission at 584 nm) was recorded at room temperature using an EnSpire® Multimode plate reader (Perkin Elmer). The Michaelis−Menten constant K_m and the maximum reaction velocity V_{max} of free STV-β-gal and STV-β-gal/Bio-hRNFs were calculated using the Lineweaver−Burk equation: $1/V = (K_m/V_{max}) \times [S] + 1/V_{max}$, where V is the initial catalytic rate, K_m is the Michaelis-Menten constant, V_{max} is the maximum catalytic rate, and [S] is the substrate concentration. The initial catalytic rate was obtained by measuring a change in fluorescence intensity of the sample and substrate only in time course.

Thermal Stability of STV-β-gal: To test the thermal stability of enzyme, free STV-β-gal and STV-β-gal/Bio-hRNFs were incubated in PBS buffer at temperatures ranging from 30 to 70 °C for 10 min. After the solution was cooled down to room temperature, the RBG substrate was added, and the fluorescence intensity was measured after 15-20 min. The relative enzymatic activity was obtained by normalizing the fluorescence signals in both free STV-β-gal and STV-β-gal/Bio-hRNFs to that of free STV-β-gal or STV-β-gal/Bio-hRNFs heated at 30 °C, respectively.

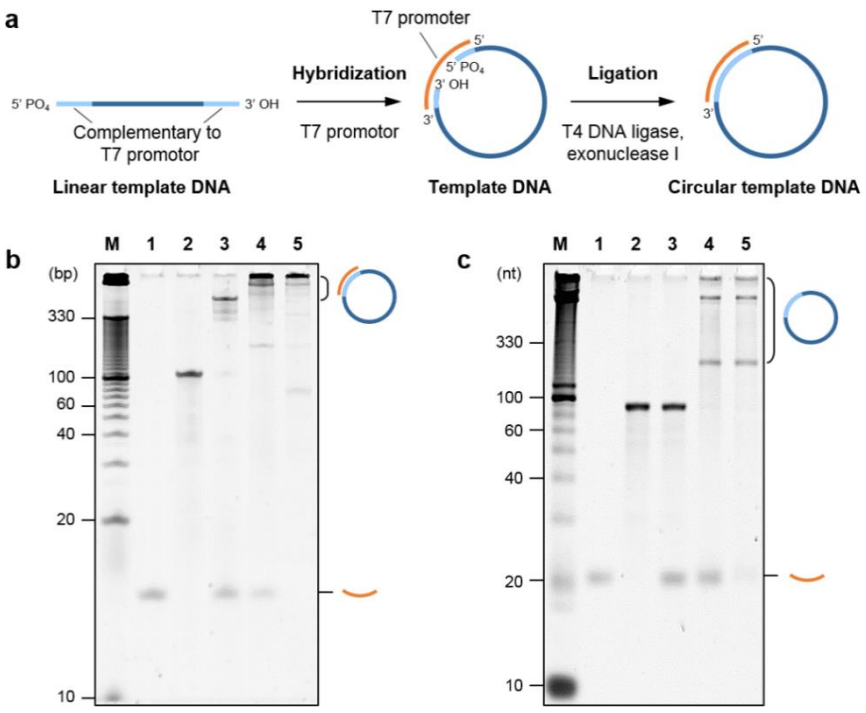

Figure S1. Circularization of linear template DNA. (a) Schematic illustration showing the preparation of circular template DNA for RCT. (b) 15% Native and (c) 15% denatured polyacrylamide gel images stained with SYBR gold. Lane M: 10 bp DNA ladder, lane 1: T7 promoter, lane 2: linear template DNA, lane 3: hybridized template DNA with T7 promoter, lane 4: template DNA after ligation with T4 DNA ligase, lane 5: circular template DNA after treatment with exonuclease I.

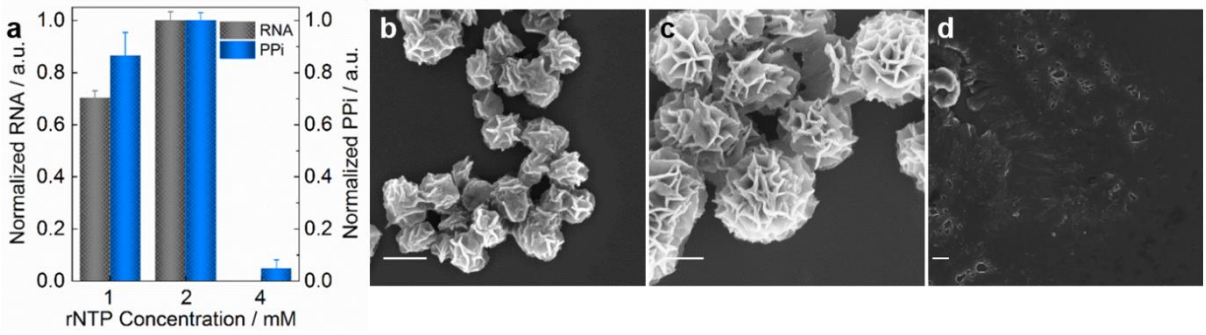

Figure S2. Optimization of the RCT reaction with varied rNTP concentrations (1, 2, and 4 mM). The concentrations of template DNA and T7 RNAP were 1 μM and 5 U/μL, respectively. (a) The RNA and PPi yield in the resulting RCT products. All the results were normalized to the value at rNTP = 2 mM. Data represent mean ± s.d. of three independent experiments. (b-d) SEM images showing the corresponding RCT products synthesized with different concentrations of rNTP: (b) 1 mM, (c) 2 mM, and (d) 4 mM. Scale bars: 500 nm. The highest amounts of RNA and PPi in hRNFs with their well-defined morphology were achieved when 2 mM rNTP was used. Further increase in rNTP (4 mM) gave rise to dramatic reduction in RNA production and no appreciable particle formation. This is presumably due to the competitive interactions between free ribonucleotides and RNAP against binding to Mg^{2+} ions, thus leading to a decrease in effective Mg^{2+} concentration required for enzyme activity.

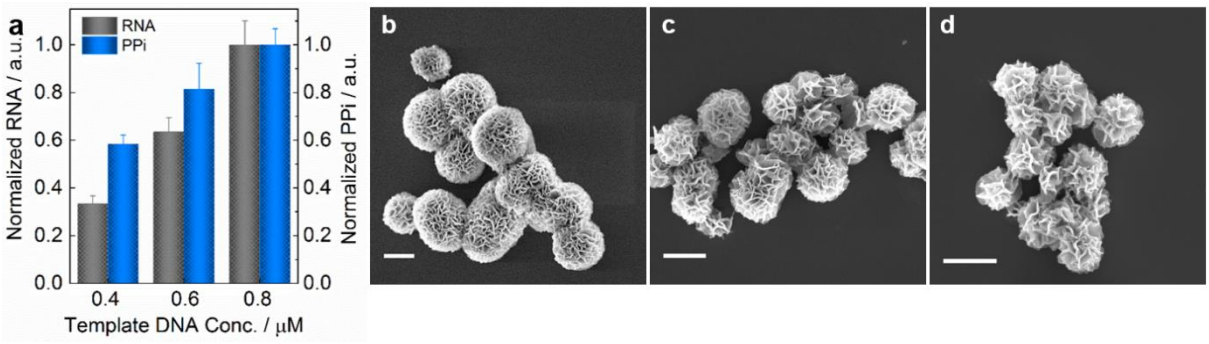

Figure S3. Optimization of RCT reaction with varied template DNA concentrations (0.4, 0.6, and 0.8 μM). The concentrations of rNTP and T7 RNAP were 2 mM and 5 U/μL, respectively. (a) The RNA and PPi yield in the resulting RCT products. All the results were normalized to the value at template DNA = 0.8 μM. Data represent mean ± s.d. of three independent experiments. (b-d) Representative SEM images of hRNFs synthesized with varied concentrations of template DNA: (b) 0.4 μM, (c) 0.6 μM, and 0.8 μM. Scale bars: 1 μm. Increasing concentration of template DNA led to a significant increase in amounts of PPi and RNA in RNFs. However, the final hRNF particles tended to be more aggregated or grown to adhere to each other when 0.8 mM or more template DNA was used.

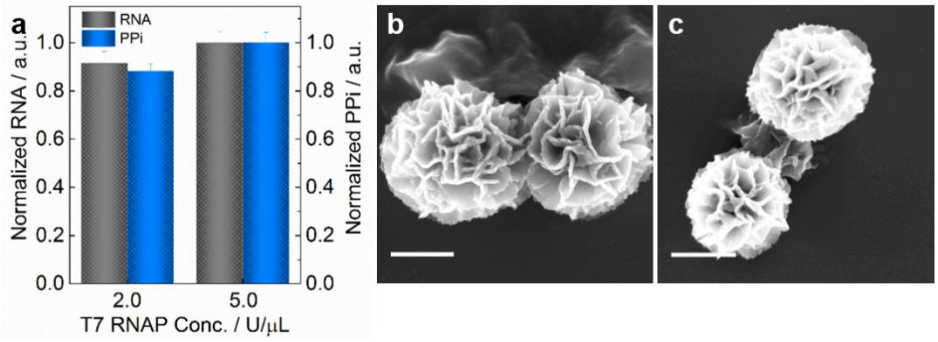

Figure S4. Optimization of the RCT reaction with different T7 RNAP concentrations (2 and 5 U/μL). The concentrations of template DNA and rNTP were 1 μM and 2 mM, respectively. (a) The RNA and PPi yield in the resulting RCT products. All the results were normalized to the value when T7 RNAP = 5 U/μL. Data represent mean ± s.d. of three independent experiments. Representative SEM of hRNFs synthesized with (b) 2 U/μL and (c) 5 U/μL of T7 RNAP. Scale bars: 500 nm. As expected, 250 units of T7 RNAP (5 U/μL) was able to yield hRNFs with higher amounts of both RNA and PPi as compared to the use of 100 units of T7 RNAP (2 U/μL).

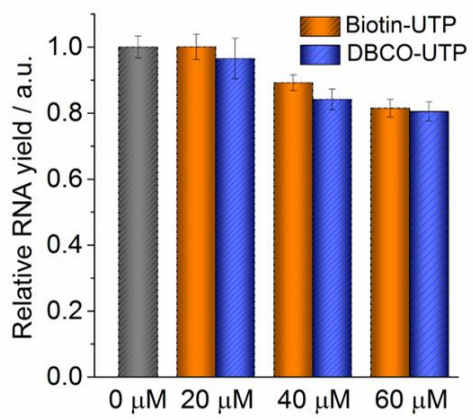

Figure S5. Optimization of the RCT reaction with increasing modified UTP. The relative RNA yields decreased with increasing the concentration of modified UTP (0, 20, 40, and 60 μM). The RNA yields of functional hRNFs (Bio-hRNFs (orange), and DBCO-hRNFs (blue)) were normalized to the RNA yield in hRNFs (grey). Data represent mean ± s.d. of three independent experiments.

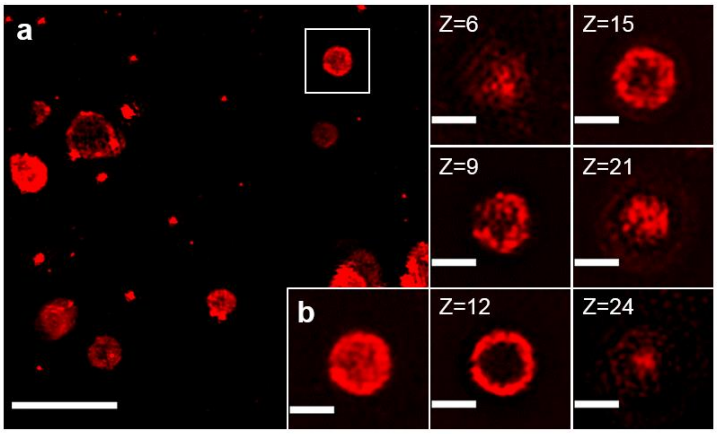

Figure S6. (a) SIM image of STV-QD_{605}/Bio-hRNFs. (b) Inset indicates a higher magnification view of the solid box in the main image. Individual frames of z-stacks of the STV-QD_{605}/Bio-hRNFs particle are shown in the right panel. Scale bars: 5 μm for the main image and 1 μm for the inset and images in the right panel.

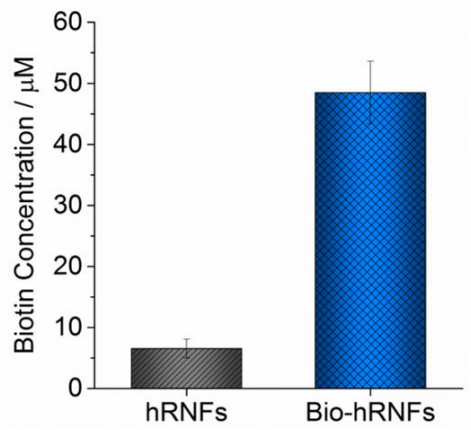

Figure S7. Determination of biotin concentration in the hRNFs and Bio-hRNFs. The presence of biotin was confirmed by measuring biotin concentration using a commercial biotin quantification kit. Data represent mean ± s.d. of three independent experiments.

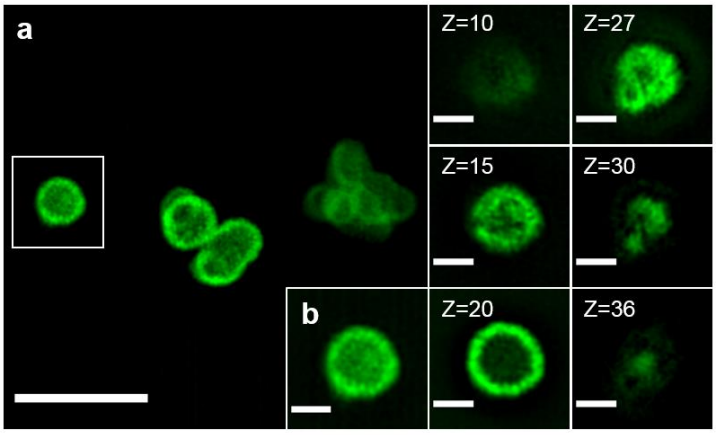

Figure S8. (a) SIM imaging of Av-AF_{488}/Bio-hRNFs. (b) Inset indicates a higher magnification view of the white box in the main image. Individual frames of z-stacks of the Av-AF_{488}/Bio-hRNFs particle are shown in the right panel. Scale bars: 5 μm for the main image and 1 μm for the inset and images in the right panel.

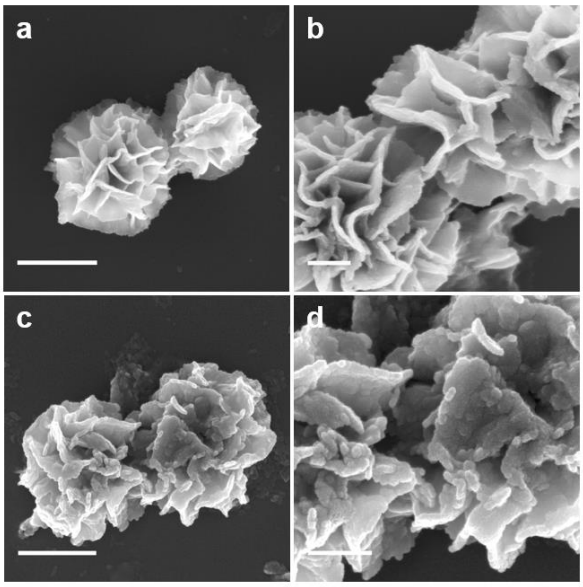

Figure S9. Coupling of the Bio-hRNFs with STV-HRP. SEM images showing the morphologies of hRNFs before and after STV-HRP coupling. (a, b) Bio-hRNFs and (c, d) STV-HRP/Bio-hRNFs conjugates. Scale bars: (a, c) 500 nm and (b, d) 200 nm.

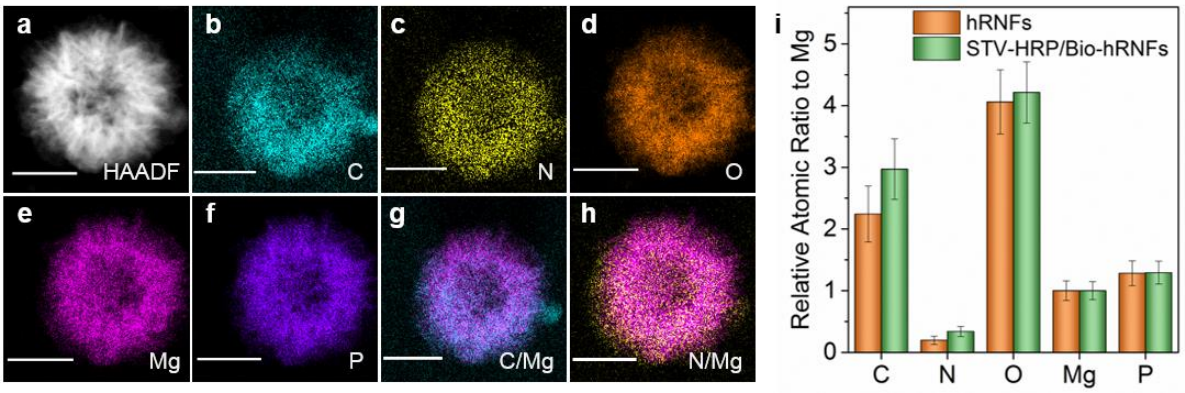

Figure S10. Characterization of the STV-HRP/Bio-hRNFs by STEM imaging and STEM-EDS analysis. (a) Representative HAADF-STEM image, and (b-h) EDS elemental maps of C, N, O, Mg, P, merged C/Mg, and N/Mg in STV-HRP/Bio-hRNFs. Scale bars: 500 nm. (i) The abundance of each element (C, N, O, and P) in the Bio-hRNFs and STV-HRP/Bio-hRNFs, as determined by STEM-EDS. The element contents of C, N, O, and P were normalized to Mg. The data represent mean ± s.d. of the EDS measurements of five particles.

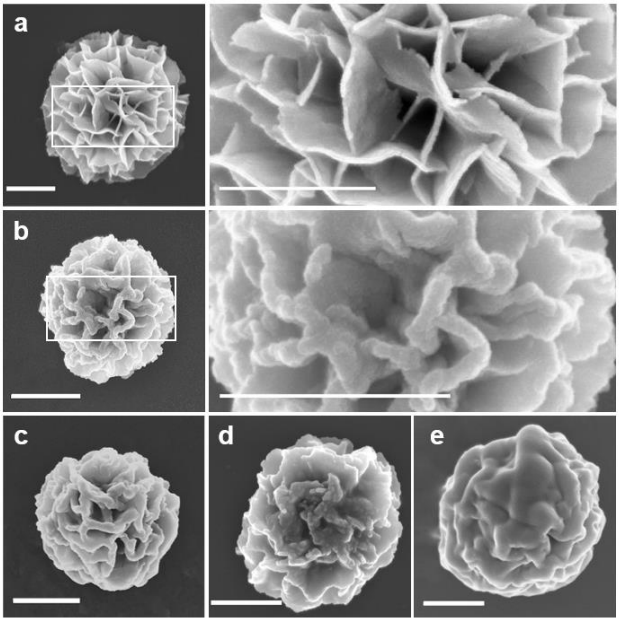

Figure S11. Functionalization of the hRNFs with avidin. Representative SEM images of the Av-hRNFs with increased avidin/RNA mass ratios: (a) 0:1, (b) 1:1, (c) 2:1, (d) 5:1, and (e) 10:1. The higher magnification views of the solid box in the main images in (a) and (b) show the increased thickness and surface roughness of the hRNF petals after coating with avidin. Scale bars: 500 nm.

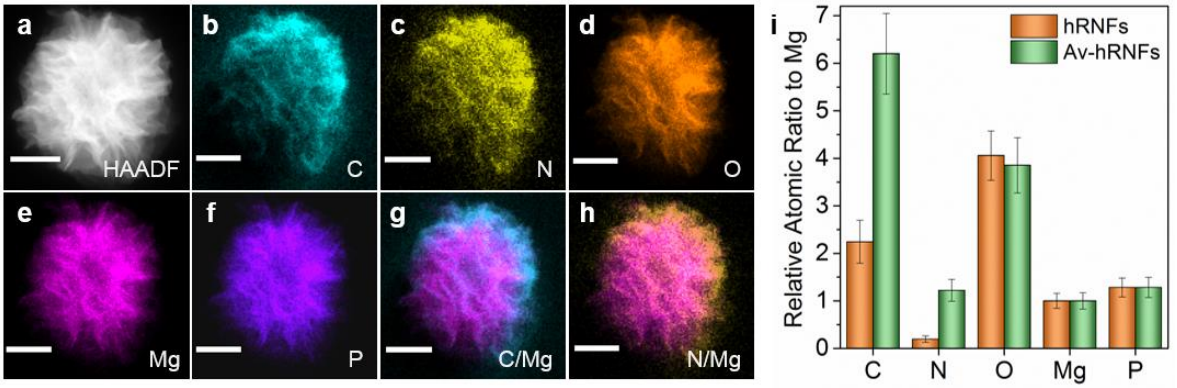

Figure S12. Characterization of the Av-hRNFs by STEM imaging and STEM-EDS analysis. (a) Representative HAADF-STEM image, and (b-h) EDS elemental maps of C, N, O, Mg, P, merged C/Mg, and N/Mg of Av-hRNFs. Scale bars: 500 nm. (i) The abundance of each element (C, N, O, Mg, and P) in the hRNFs and Av-hRNFs as determined by STEM-EDS. The element contents of C, N, O, and P were normalized to Mg. Data represent mean ± s.d. of the EDS measurements of five particles.

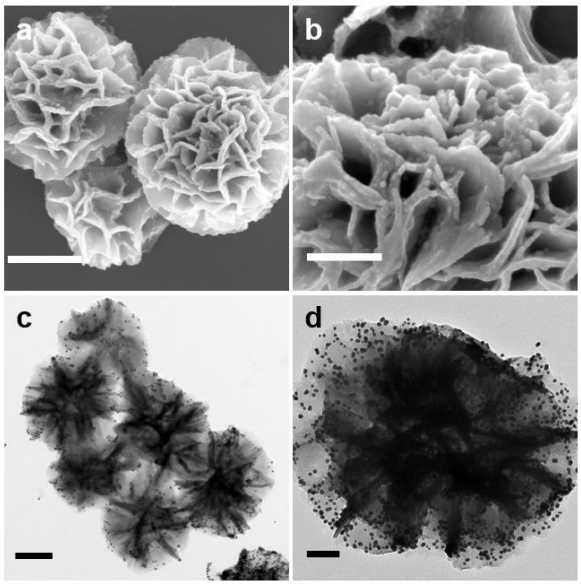

Figure S13. Representative (a, b) SEM and (c, d) TEM images of the Bio-GNPs/Av-hRNFs. Biotin conjugated gold nanoparticles (Bio-GNPs) were well distributed on Av-hRNFs, indicating that positively-charged avidin molecules are presumably attached onto negatively-charged RNA on the periphery of the Av-hRNFs. Scale bars: (a, c) 500 nm and (b, d) 200 nm.

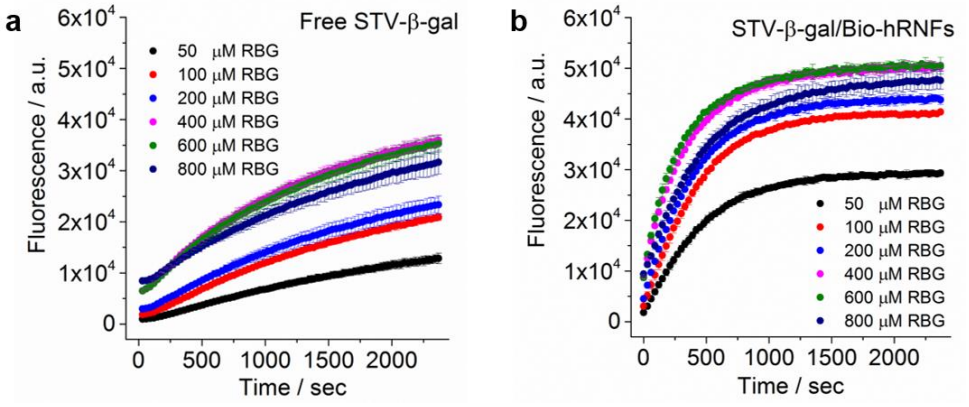

Figure S14. The hydrolysis kinetics of RBG substrate catalyzed by (a) free STV-β-gal and (b) STV-β-gal/Bio-hRNFs. The concentration of RBG substrates ranges from 50 to 800 μM. The enzyme concentration was 200 ng/mL. The hydrolytic product was monitored with the fluorescence at an excitation of 550 nm and emission of 584 nm. Data represent mean ± s.d. of three independent experiments.

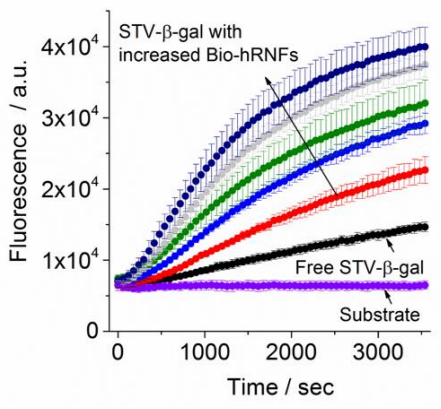

Figure S15. Effect of Bio-hRNFs on the enzymatic activity of STV-β-gal. STV-β-gal (100 ng/mL) was incubated with varied Bio-hRNFs (0, 2, 4, 6, 8, and 10 μg/mL). The hydrolytic product was monitored after adding RBG substrates (200 μM) with the fluorescence at an excitation of 550 nm and emission of 584 nm. Data represent mean ± s.d. of three independent experiments.

References:

(1) Wang, Y.; Howes, P. D.; Kim, E.; Spicer, C. D.; Thomas, M. R.; Lin, Y.; Crowder, S. W.; Pence, I. J.; Stevens, M. M. Duplex-Specific Nuclease-Amplified Detection of MicroRNA Using Compact Quantum Dot–DNA Conjugates. *ACS Appl. Mater. Interfaces* **2018**, *10*, 28290-28300.

(2) Kim, E.; Zwi-Dantsis, L.; Reznikov, N.; Hansel, C. S.; Agarwal, S.; Stevens, M. M. One-Pot Synthesis of Multiple Protein-Encapsulated DNA Flowers and Their Application in Intracellular Protein Delivery. *Adv. Mater.* **2017**, *29*, 1701086.